Skin Friction Measurements by Laser Interferometry in Swept Shock/Boundary-Layer Interactions

Kwang-Soo Kim* and Gary S. Settles†
Pennsylvania State University, University Park, Pennsylvania

Measurements have been made of wall shear stresses in swept interactions of planar shock waves generated by a sharp fin and the two-dimensional turbulent boundary layer on a flat plate. Test conditions were Mach number 3.03, Reynolds number $Re_\theta \simeq 1.5 \times 10^4$, wall temperature near adiabatic, and fin angles of 10 and 16 deg. Measurements were made using the Laser Interferometer Skin Friction (LISF) meter, which optically detects the thickness of an oil film on the test surface. The results show that such measurements are practical in high-speed interacting flows with a repeatability of ± 12% or better. Further, with proper data handling, LISF measurements appear feasible at very high shear levels, which were previously considered unobtainable. Dramatic increases in wall shear were observed in both swept interactions tested. These data are compared with computational Navier-Stokes solutions by Horstman and Knight wherein k-ϵ and algebraic turbulence models were used. Both computations predict the overall measured c_f levels at $\alpha = 10$ deg but fail to predict some features of the c_f distributions properly.

Nomenclature

c_f = skin friction coefficient based on incoming freestream conditions
M_∞ = incoming freestream Mach number
N = number of fringes
p_o = stagnation pressure of incoming stream, MPa (psia)
p_w = wall static pressure on flat plate, MPa (psia)
p_∞ = incoming freestream static pressure, MPa (psia)
R = radial distance measured from the fin leading-edge, cm (in.)
Re_θ = Reynolds number based on the local, undisturbed boundary-layer momentum thickness
s = distance measured along surface streamline, mm
T_{aw} = adiabatic wall temperature, K
T_o = freestream stagnation temperature, K
T_w = wall temperature, K
u^+, y^+ = dimensionless wall-wake velocity and height coordinates
x,y,z = orthogonal streamwise, normal, and spanwise coordinates, respectively, cm
α = angle made by fin with respect to the incoming freestream direction, deg
β = angle with respect to freestream direction, measured from fin leading edge, deg
Δs = distance from oil-film leading edge to laser spot along surface streamline, mm
δ = local, undisturbed boundary-layer thickness, mm
ν = oil viscosity, cs
Π = boundary-layer, wake-strength parameter
τ_w = wall shear stress, N/m^2

Subscripts

is = incident shock wave location
ps = primary separation line location
r = reattachment line location
ss = secondary separation line location
ui = upstream influence line location

Introduction

SWEPT shock wave/boundary-layer interactions are among the chief aerothermodynamic problems that currently limit high-speed propulsion and flight. They also represent a fundamental problem area of modern fluid dynamics which has, thus far, evaded any comprehensive theoretical or computational treatment. Many publications and a recent survey article[1] have appeared on this subject.

The computation of complex viscous-inviscid interacting flows such as the swept shock/boundary-layer interaction is presently paced by the need for detailed, "benchmark" experiments for code validation.[2] In particular, it is widely recognized that traditional measurements such as surface pressures and oil flows are inadequate for this purpose. The current state-of-the-art Navier-Stokes solvers still employ highly simplified turbulence models whose efficacy is in considerable doubt for complex interacting flows. Experimental data that directly address the turbulent stresses in these flows are sorely needed to advance both the development and validation of turbulence modeling. Unfortunately, such experiments are difficult and expensive to perform in high-speed flows.

Recognizing this, the participants of the 1980-81 AFOSR-HTTM-Stanford Conference on Complex Turbulent Flows scrutinized the available data base and recommended certain directions for future experimentation.[3] Among these was the suggestion that detailed and accurate heat transfer and skin friction data be obtained in high-speed flow experiments. These quantities, being directly linked to turbulent stresses within the boundary layer, provide a more significant level of comparison with computational fluid dynamics (CFD) results than do, for example, surface pressures. However, heat transfer and especialy skin friction are difficult to measure with acceptable accuracy in high-speed interacting flows.

The traditional methods for the measurement of skin friction in high-speed flows have been thoroughly reviewed by Winter.[4] Recent developments were also surveyed by Settles.[5]

Presented as Paper 88-0497 at the AIAA 26th Aerospace Sciences Meeting, Reno, Nevada, Jan. 11-14, 1988; received April 4, 1988; revision received March 2, 1989.

*Graduate Research Assistant, Mechanical Engineering Department; (currently, National Research Council Research Fellow, NASA Ames Research Center, Moffett Field, CA). Member AIAA.

†Professor, Mechanical Engineering Department and Director, Gas Dynamics Laboratory. Associate Fellow AIAA.

Other than the direct measurement of wall shear stress τ_w, by a balance, the available techniques infer skin friction from some other measured quantity such as heat transfer or pitot pressure. The validity of such inferential methods is doubtful in complex interacting flows. Further, floating-element balances have serious problems in such flows due to pressure gradients and poor spatial resolution. Thus, for the class of flows in question, reliable measurement techniques have been essentially nonexistent. As a result, there are no known skin friction data in shock/boundary-layer interactions of acceptable accuracy for code validation purposes.

A recent development, the Laser Interferometer Skin Friction (LISF) meter, promises to resolve this problem. The LISF meter was invented by Tanner and Blows[6] and was subsequently refined by Tanner,[7] Monson and Higuchi,[8] Monson et al.,[9,10,11] Westphal et al.,[12] and Kim and Settles.[13] It interferometrically senses the time rate of thinning of an oil film on a polished surface subjected to aerodynamic shear. In two-dimensional (2-D) flows without pressure gradients, oil lubrication theory then gives τ_w directly, without reference to the properties of the overlying boundary layer. While some corrections may be required in pressure-gradient and shear-gradient flows, the instrument nonetheless delivers essentially a direct measurement of τ_w. The Pennsylvania State University version of this instrument and its associated data handling procedures[13] is believed to be the only compressible-flow LISF meter currently in existence.

The applicability, repeatability, and accuracy of the LISF technique for use in compressible flows have been determined by Kim and Settles[13] through an experimental calibration over a range of Mach numbers. This calibration was done using zero-pressure-gradient turbulent boundary layers. It revealed the mean LISF skin friction value to be about 8% low at Mach 2.5, improving to only 3% low at Mach 4 (presumably in part due to an improvement in the LISF fringe count at higher Mach numbers). It was also observed that surface-wave phenomena on the oil film limit the technique in high-τ_w flows, but this does not preclude accurate measurements in the supersonic Mach number range. Monson[10] measured a maximum level of $\tau_w = 120$ N/m^2 with the LISF meter in high-Reynolds number supersonic flow. Here, we extend that limit to almost 600 N/m^2.

The present paper reports an experimental study in which the LISF meter is used to measure τ_w distributions in two interactions of fin-generated, swept shock waves with turbulent boundary layers. The basic research configuration is an unswept, sharp-leading-edge fin of variable angle α mounted on a flat plate. This configuration generates "building-block" interactions representative of those occurring on practical high-speed vehicles. Two examples are fin-fuselage junctions and corner flows in supersonic engine inlets.

The goal of this study is to apply the LISF meter to obtain reliable τ_w data in three-dimensional (3-D) swept shock wave/turbulent boundary-layer interactions. Such data are sought in order to shed light on the physical mechanisms of such interactions and to provide a benchmark for CFD code validation. In particular, the data are expected to be useful in judging the effectiveness of current turbulence models.

Experimental Methods

Wind Tunnel and Test Conditions

The Pennsylvania State University Supersonic Wind Tunnel[14] used in this study is a blowdown facility with a nominal Mach number range of 1.5–4. The variable-Mach-number capability is achieved by way of an asymmetric sliding-block nozzle. The test section of the wind tunnel is 150 mm (6 in.) wide, 165 mm (6.5 in.) high, and 610 mm (24 in.) long. Calibration experiments have revealed good flow quality across the available Mach number range. Wind tunnel run durations for the present study ranged from 20–30 s.

The test Mach number was fixed at 3.03 ± 0.033 in this study. The stagnation conditions of the flow were $p_0 = 0.827$ MPa (120 psia) $\pm$ 3.9% and $T_0 = 293.5$ K $\pm$ 2.7%, yielding a freestream unit Reynolds number of 6.19×10^7/m $\pm$ 4%.

The interaction test surface was a flat plate, 500 mm (19.5 in.) long, which spanned the test section. Natural boundary-layer transition was observed to occur within 2 cm of the plate leading edge. The plate was fitted with both surface-pressure taps and surface thermocouples. An unswept fin shock generator was positioned with its sharp leading edge 216 mm (8.5 in.) from the plate leading edge and 26.2 mm (1.03 in.) from the tunnel sidewall. The fin was 100 mm (4 in.) high, 127 mm (5 in.) long, and 6.35 mm (0.25 in.) thick. The fin height of about 30δ insured that the interaction was a semi-infinite one for the region of the interaction under present study.[1] A sketch of the fin/plate test configuration is shown in Fig. 1.

The fin angle of attack was varied by a pneumatic fin-injection mechanism mounted through the tunnel sidewall. The bottom of the fin had a rubber seal which insured that no leakage under the fin occurred during the experiments. Two fin angle of attack values, $\alpha = 10$ and 16 deg, were tested. The fin angles were determined to 0.1 deg accuracy using a machinist's protractor.

The flat plate contained 96 surface-pressure taps arranged in concentric circular arcs about the fin leading-edge position. This arrangement was chosen to take advantage of the quasi-conical interaction symmetry that has been fully described elsewhere.[1] The pressure-tap arc radii were multiples of 25.4 mm (1 in.). LISF measurements were also made along circular arcs centered about the fin leading edge. However, these were chosen midway between the pressure-tap arcs in order to avoid interference. For the $\alpha = 10$ deg case, the arc radius R for LISF measurements was 114.3 mm (4.5 in.). The R was reduced to 88.9 mm (3.5 in.) for $\alpha = 16$ deg in order to avoid possible interference due to the shock-wave interaction with the wind tunnel sidewall boundary layer. Finally, some additional LISF data were taken along radii from the conical-flow virtual origin. These radii lay at $\beta = 24$ deg for the $\alpha = 10$ deg case and $\beta = 38$ deg for the $\alpha = 16$ deg case.

The undisturbed flat-plate boundary layer has been surveyed and documented[14] for test conditions close to those of the present study (same M_∞, but Re_θ 11% lower than present). Pitot-pressure surveys along the flat-plate centerline and 38 mm (1.5 in.) to each side showed that the test boundary layer is 2-D, turbulent, and in equilibrium in the sense that it satisfies the combined law of the wall/law of the wake with constant Π within the accepted equilibrium range. The test boundary-layer is also near-adiabatic ($T_w/T_{aw} = 1.06 \pm 2.2\%$). The mean velocity profile of the undisturbed boundary layer at $x = 28$ cm (11 in.) from the flat plate leading edge is shown in Fig. 2, along with the corresponding Sun-Childs[15] compressible wall-wake curve fit. The boundary-layer parameters extracted from this curve fit are: $\delta = 4.4$ mm,

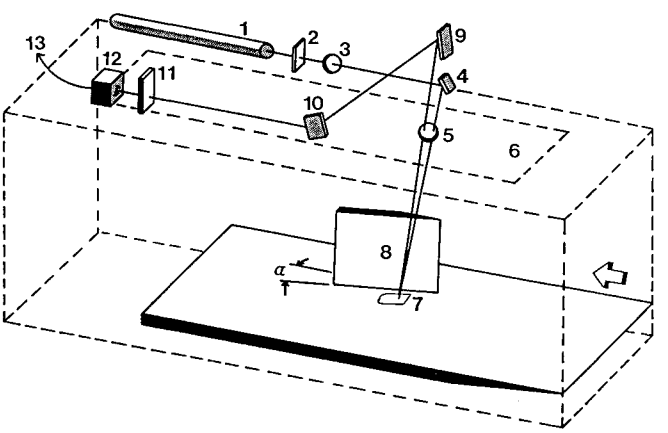

Fig. 1 Schematic diagram of LISF meter, flat plate, and fin (see text for key).

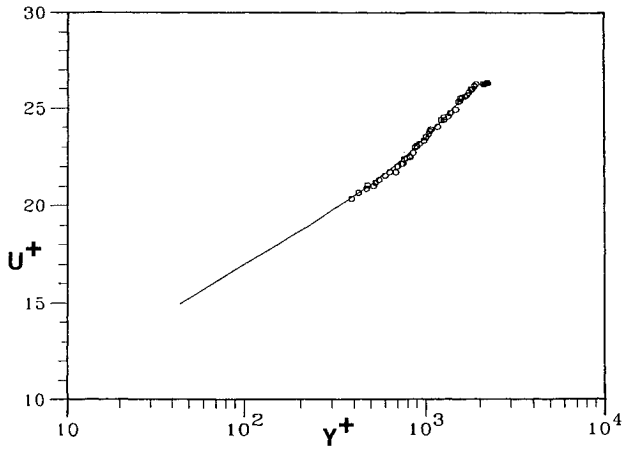

Fig. 2 Incoming velocity profile wall-wake curve fit.

$Re_\theta = 1.3408 \times 10^4$, $\Pi = 0.63$, and $c_f = 0.0015$. For the higher $Re_\theta = 1.4915 \times 10^4$ of the present study, c_f in the incoming boundary layer is predicted to be 0.0014 by the Van Driest II theory.[16]

LISF Meter in High-speed 3-D Flow

The underlying theory of the LISF technique and examples of its application, mainly in incompressible flows, are thoroughly documented in Refs. 6–12. The adaptation of the LISF meter for use in compressible flows has further been discussed in detail by Kim and Settles.[13] The major limitation of the technique is due to surface-wave phenomena on the oil film in high-τ_w flows, about which more will be said below.

Other than in a supersonic delta-wing demonstration experiment by Monson et al.,[9] the LISF meter has not been used in compressible 3-D flows prior to the present study. One of our goals is to establish firmly the applicability of the instrument to such flows.

It is generally necessary in 3-D LISF measurements to know the direction of the τ_w vector a priori, since an accurate knowledge of the distance Δs from the oil-film leading edge to laser-beam measuring spot is required. Alternatively, when the dual-beam LISF adaptation is used,[8-12] Δs need not be measured. However, in that case either the dual beam spots must still be aligned with the local τ_w direction, or two components of τ_w must be measured with considerable extra effort.

Local τ_w directions may be determined directly from surface-flow visualization results, assuming that these are obtained in a quantitative manner. It is known that small-amplitude broadband fluctuations occur in shock wave/turbulent boundary-layer interactions though the overall flow structure has been observed to be nominally stationary. Since surface-flow visualization methods have little or no frequency response, they clearly perform some sort of averaging process. In the absence of evidence to the contrary, we have assumed that such patterns yield a true representation of the local mean direction of the τ_w vector.

The kerosene-lampblack-adhesive tape technique[17] is particularly suitable for determining τ_w directions, in that it yields undistorted, full-scale, surface-streak patterns. Angular measurements of local τ_w directions are possible with ± 0.5 deg routine accuracy. Such patterns were obtained for the $\alpha = 10$ and 16 deg test cases of the present study and are shown in Fig. 3. During LISF tests, full-scale transparent overlays of these surface-flow patterns were used to identify the surface-flow direction corresponding to a given position of the laser-beam measuring spot.

After applying the oil film to the flat plate, an optical cathetometer (least count: 0.025 mm) aligned normal to the surface-flow direction was used to measure Δs with a repeatability of $\pm 0.6\%$. The leading edge of the oil film was highlighted for this purpose by reflected light from a spotlight positioned outside the wind tunnel. Still, uncertainty of the exact oil-film, leading-edge position was the major contributor to uncertainty in Δs. Checks were made to insure that Δs did not shift due to wind tunnel startup. With practice, Δs was measured with an overall accuracy of $\pm 2\%$.

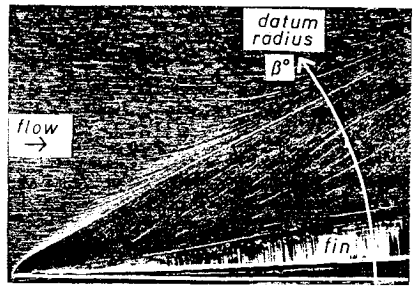

Fig. 3a Kerosene-lampblack surface-flow pattern for $\alpha = 10$ deg.

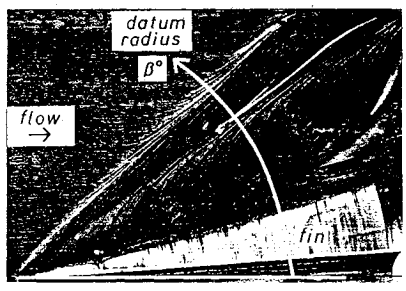

Fig. 3b Kerosene-lampblack surface-flow pattern for $\alpha = 16$ deg.

With this technique to obtain accurate Δs measurements along the local surface-flow directions, we were able to use the single-beam LISF-meter arrangement shown in Fig. 1. The dual-beam method, originally developed from the single-beam method by Monson and colleagues, was a solution to the problem of inaccuracy in measuring Δs. Its advantages lie in overcoming problems due to poor optical access, wind tunnel motion during startup, and possible spreading of the oil film after Δs is measured. However, for 3-D flows the dual-beam approach appears to involve added complexity and mechanical alignment difficulties that outweigh these advantages. With the simpler single-beam method, there is no basic difference in the LISF technique for 2-D and 3-D flows.

Arrangement of LISF Meter and Data Acquisition System

Figure 1 illustrates the components of the single-beam LISF meter used in this study. The beam from a 5-mW, linearly polarized, helium-neon laser (1) first passes through a 50% neutral-density filter (2) and an iris diaphragm (3). The beam is then directed downward by a folding mirror (4), and focused by a lens (5), passing through the plexiglas ceiling window (6) of the wind tunnel to form a spot of about 450 μm diam at an appropriate point (7) on the flat plate. During experiments, a thin film of $\nu = 500$ cS Dow-Corning "200" silicone oil applied to a local region (7) of the flat plate is sheared by the τ_w distribution of the shock/boundary-layer interaction due to the fin (8). The incident laser beam is reflected by both the surface of the oil film and the polished plate beneath it. This produces a reflected, two-component, interfering laser beam directed out of the wind tunnel through the ceiling window. (The beam angles of incidence and reflection are kept to about 1 deg.) The reflected beam is intercepted by two first-surface aiming mirrors, (9) and (10), where it is directed through a ground-glass diffuser (11) and a 6328 Å filter onto a photodiode (12).

The photodiode senses a time-dependent light intensity due to the interference of light reflected from the oil film and test surface. The photodiode output (13) is raised to a level of 8 V

by an internal operational amplifier, low-pass filtered with a 10-Hz cutoff to remove high-frequency, vibration-induced optical noise above the oil-film response range, and recorded. Seven other channels of data are recorded simultaneously: p_0, T_0, two p_w channels, and three T_w channels. The data channels are simultaneously sampled by a multiplexer, digitized by a microcomputer-controlled analog/digital converter, and stored in the computer memory. For present purposes, a 20-Hz data rate was initially chosen, yielding at least 20 points per interference fringe. However, the requirement for greater accuracy in high-shear regions of the flow led to an increase of the data rate to 50 Hz. The photodiode output was also monitored in real time on a strip-chart recorder during the experiments.

Data Reduction

A detailed account of LISF data reduction procedures is given by Kim and Settles.[13] Briefly, the limited fringe count obtainable in high-τ_w flows calls for somewhat different data reduction than that reported by other investigators for incompressible flows. Given only 2-8 fringes, it becomes necessary to determine τ_w based on the entire signal within the usable fringe record. Merely determining the time interval corresponding to 3 arbitrary fringe peaks (minima and maxima), as is done in incompressible flow, does not yield sufficient accuracy here.

Thus, as described in Ref. 13, it is necessary to define that part of the fringe record which is usable and consistent with oil lubrication theory, i.e., which conforms to a regular "envelope." The initial and final segments of the fringe record which do not so conform are discarded as are occasional distorted fringe records due to dust particles on the oil film, etc. Usable fringe records are smoothed by repeated application of an adjacent-point averaging algorithm until all noise on the signal is removed.

The LISF data reduction equation,[8] derived from the Navier-Stokes equation and assuming constant wall shear stress, is

$$\tau_w = \frac{2n\rho\nu\cos(r)}{\lambda}\left[\frac{\Delta s}{N't'}\right] \tag{1}$$

where N' = effective fringe number, t' = effective oil-flow time, n = oil refractive index, ρ = oil density, λ = laser wavelength, and r = oil refraction angle.

Equation (1) requires a correction for the effect of variable T_w on ν, as described in Ref. 13. This correction is critical to LISF measurements in high-speed flows since a 1°C change in T_w causes about a 2% change in ν. Accordingly, the viscosity-temperature characteristics of a sample of 500-cS silicone oil were determined by a professional testing laboratory to an accuracy of better than 1% over the present temperature range.

The calculation of N' and t' in Eq. (1) is carried out following Eqs. (6) and (7) of Ref. 13. These results are next compared with oil lubrication theory in the N'-t' plane as shown in Fig. 4 for a case where $\tau_w = 577$ N/m^2. A least-squares curve fit of the data to the lubrication theory is performed, followed by a computation of the reduced deviation of the data from the fitted curve, χ^2_ν, which is defined as χ^2 divided by the number of degrees of freedom. Then, the first fringe peak (i.e., the first data point) is eliminated, and the fit is repeated since more fringe peaks do not always lead to greater accuracy. This process is continued up to $\Delta N = -1.5$, rather than -2 as quoted in Ref. 13, considering the small number of usable fringes in the present study, due to high τ_w, as compared to our previous work. The value of $N't'$ corresponding to the curve fit with the minimum χ^2_ν is used in the calculation of τ_w in Eq. (1).

Before τ_w is found, however, two further corrections[8,9] are required in principle, since the oil film in the present experiments is subject to both pressure and shear gradients. The pressure-gradient correction[8] was evaluated through interpolation of p_w measured at the radial tap rows on either side of the LISF measurement arc on the flat plate. These pressure distributions, obtained in an earlier study,[14] are plotted in Fig. 5 as functions of the angle β. Note that it was deliberately chosen to take LISF data in the region of quasiconical interaction symmetry well downstream of the fin leading edge. Thus, as shown in Fig. 5, p_w vs β is essentially independent of R.

The pressure-gradient correction for the present experiments amounted at most to $\pm 0.1\%$, which is negligible. This fact is significant in that pressure-gradient errors are controlling factors in most other methods of skin friction measurement.[4,5] However, it cannot be stated categorically that the LISF pressure-gradient correction will always be negligible in all experiments. Two-dimensional interactions, for example, could produce pressure gradients large enough to make this correction significant.

The shear-gradient correction[9] is quite simple for the single-beam LISF technique. The correction is required if there is a significant change in τ_w from the oil-film, leading-edge to the laser-beam measurement spot. This correction has the form

$$\tau_w' = \tau_w + \frac{1}{4}\frac{\partial\tau_w}{\partial s}\Delta s \tag{2}$$

where τ_w' = the corrected value of wall shear stress. For small Δs, one may assume that $\partial\tau_w/\partial s$ = a constant locally. Thus the correction is accomplished by a shift of the measurement point along the surface streamline direction. However, for the present experiments, $\Delta s \simeq 2$ mm; therefore, the required shift is only $\simeq 0.5$ mm, which is negligible. In general, a shear-gradient correction may always be avoided in single-beam LISF measurements if Δs is kept small.

Error Analysis

The uncertainties in the flow quantities and other parameters connected with the LISF measurements have been cited in

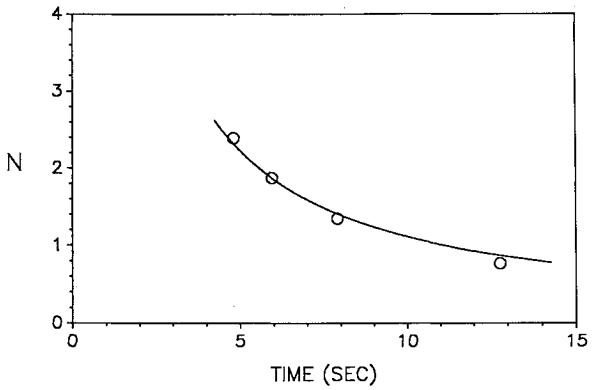

Fig. 4 Fringe number vs time for $\tau_w = 577$ N/m^2.

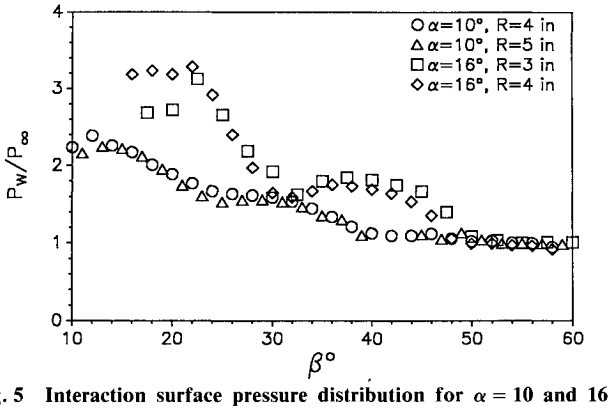

Fig. 5 Interaction surface pressure distribution for $\alpha = 10$ and 16 deg.

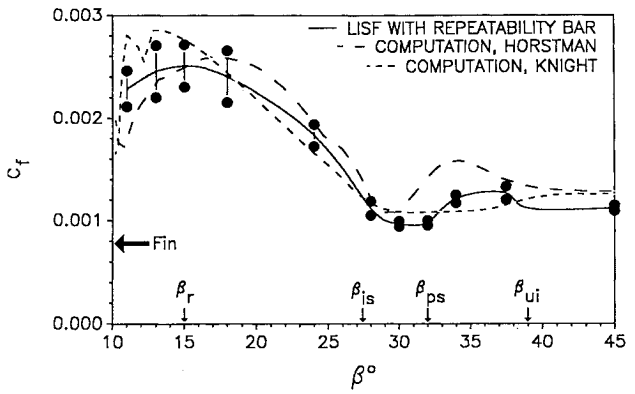

Fig. 6 The c_f distribution for $\alpha = 10$ deg with CFD comparison.

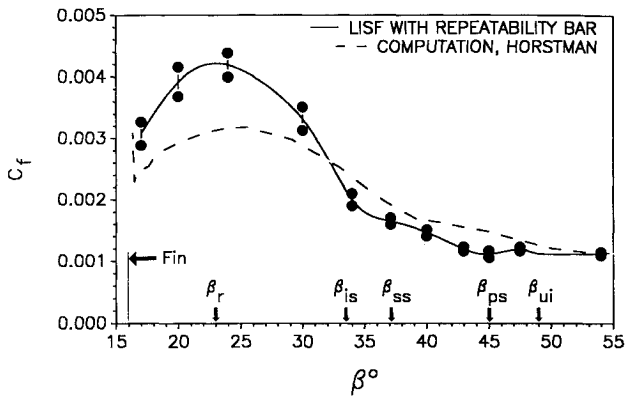

Fig. 7 The c_f distribution for $\alpha = 16$ deg with CFD comparison.

previous sections. In all cases, these uncertainties are given as the mean value ± two standard deviations. Each measurement point within the two swept interactions studied here was repeated seven times in separate wind tunnel runs. Gaussian distributions resulted. Chauvenet's criterion was then applied once to each seven-point ensemble to discard, if necessary, a single bad point from the ensemble. The error bars in the plots of the following sections indicate the repeatability of the data as ± 2 standard deviation about the mean. In general, the repeatability error varied from as little as ± 4% upstream of the interaction to as much as ± 20% at the highest τ_w in the $\alpha = 10$ deg case. In the subsequent $\alpha = 16$ deg experiments, a higher data acquisition rate and experience combined to limit the repeatability band to ± 12% or less.

Of course, there exists no calibration standard with which to judge the absolute accuracy of τ_w measurements in shock/boundary-layer interactions. However, the accuracy of LISF measurements in compressible, flat-plate, turbulent boundary layers has been assessed in previous calibration experiments.[9,13] By coming to terms with the limits imposed by high shear levels on the usable fringe count, the error band has been reduced from ± 20%[9] to ± 12%[13] at the Mach number of the present study. As discussed below, further improvements may be possible.

Results and Discussion

The measured skin friction distribution for $\alpha = 10$ deg, $R = 114.3$ mm (4.5 in.) is shown in Fig. 6. As in Fig. 5, the c_f data are plotted vs the angle β measured from the fin leading edge since the interaction is quasiconical. The flat-plate c_f level ahead of the interaction is 0.0011, which is 20% below the value predicted by the Van Driest II theory.[16] (The reason for this is unknown, since our calibration experiments[13] showed only a 6% disagreement with Van Driest at Mach 3.)

At the upstream-influence line of the interaction ($\beta = 39$ deg), c_f initially rises, then falls again in the region between the separation line ($\beta = 32$ deg), and the angle of the inviscid fin-shock wave ($\beta = 27.4$ deg). From this location aft to $\beta = 15$ deg, a steep rise in c_f occurs, reaching maximum values of 0.0025 or 230% of the incoming level. Finally, c_f decreases slightly as the fin ($\alpha = \beta = 10$ deg) is approached.

Our physical interpretation of the measurements shown in Fig. 6 is as follows. The initial rise of c_f at the upstream influence line appears to be due to the onset of the swept pressure gradient, which shears the bottom of the incoming boundary-layer in the spanwise direction. Low-momentum fluid is thus removed from the boundary-layer, such that the velocity-gradient normal to the surface (and thus c_f) is increased. The onset of the swept interaction may therefore be imagined as a natural boundary-layer control mechanism. However, separation nonetheless occurs downstream where the convergence of upstream and downstream fluid at the wall reduces the normal velocity gradient and c_f. The steep rise to maximum c_f values near the fin is explained in terms of recent structural studies of separated fin interaction flowfields.[18] The observed "λ-shock" structure causes the impingement of a high-speed jet on the flat plate in the vicinity of the line of flow reattachment near the fin. This phenomenon is known to produce very high τ_w, p_w, and heat transfer levels.[19] From this jet impingement region, the fluid near the wall moves spanwise and forward to eventually meet the separation line. Thus the phenomenology of the region 15 deg $\leq \beta \leq$ 32 deg in Fig. 6 is a rapid decrease of c_f from its maximum level as the separation line is approached from behind.

The measured skin friction distribution for $\alpha = 16$ deg, $R = 88.9$ mm (3.5 in.) is shown in Fig. 7. This stronger interaction exhibits the same qualitative c_f features as the 10-deg case. However, the maximum c_f level is now 0.0041, or 370% higher than the incoming boundary-layer c_f. As the interaction strength grows, the jet-impingement phenomenon described above also grows stronger and produces higher local wall shear, here centered about $\beta \simeq 24$ deg. The skin friction drops rapidly and almost symmetrically on either side of this impingement region.

The initial rise in c_f at the upstream-influence line, prominent in Fig. 6, is almost unnoticeable in Fig. 7. Here the upstream influence line lies at $\beta = 49$ deg and the separation line occurs at $\beta = 45$ deg, i.e., very close together. Previous studies[1,20] have shown that the angular increment between upstream influence and separation decreases with increasing interaction strength, eventually becoming quite small. Thus the initial rise in c_f at the interaction onset is judged to be primarily a weak-interaction phenomenon.

Between the inviscid shock location ($\beta = 33.3$ deg) and the separation line, c_f decays less rapidly than in its steep fall from the jet-impingement location at $\beta \simeq 24$ deg. Within this region at $\beta = 37$ deg lies a surface-flow feature commonly referred to as "secondary separation," which is quite weak in the present case (see Figure 3b). No indication of its presence is noticeable in the c_f distribution. However, measurements now in progress in even stronger interactions do show a distinct peak in c_f just upstream of the secondary separation line.

Throughout these experiments, the performance of the LISF meter was quite consistent with previous experience in simpler flows.[13] The primary noticeable difference in performance was due to high interaction shear levels which produced fewer usable fringes than before. However, for laser-beam spot locations directly beneath the incident shock, noisy fringe signals were obtained. This is thought to result from laser-beam refraction by the shock when the two are essentially coplanar. Even so, it was possible to filter out the noise and still obtain a c_f measurement beneath the shock.

Comparison with Navier-Stokes Computations

Computational simulations have been carried out by Knight et al.[21] for swept, fin-generated interactions with essentially the same boundary conditions as in the present experiments.

These investigators provided the detailed results of their computations[22,23] for comparison with our measured c_f distributions. In all cases, the compressible, Reynolds-averaged Navier-Stokes equations were solved, though different numerical algorithms, grids, and turbulence models were used. Horstman's solutions employed the Jones-Launder, two-equation k-ϵ turbulence model, and Knight used the Baldwin-Lomax algebraic eddy-viscosity turbulence model. A detailed description of these computations is omitted here due to space limitations but is thoroughly documented elsewhere (e.g., Ref. 21).

A comparison of the Horstman and Knight CFD results with the present $\alpha = 10$ deg c_f data is shown in Fig. 6. [Note that an interpolation of the computed mesh points of both computations was done by the present authors in order to present all results at $R = 114.3$ mm (4.5 in.) from the fin leading edge.] Both computations reasonably predict the high measured c_f level around $\beta = 15$ deg, as well as its decay with increasing β. However, Knight's result shows as initial decrease in c_f near the beginning of the interaction whereas an increase was measured. Horstman's solution slightly overpredicts this increase. Overall, Horstman's k-ϵ solution best predicts the LISF measurements.

A comparison of the Horstman's CFD result with the present $\alpha = 16$ deg c_f data is shown in Fig. 7. (No computation for this fin angle was carried out by Knight.) The upstream initial c_f rise is slightly overpredicted, compared with the measurements. Horstman's solution underpredicts our measurements aft of the inviscid shock location at $\beta = 33.3$ deg by up to 30%.

Finally, the additional LISF data taken along radii from the quasiconical virtual origin at $\beta = 24$ deg for the $\alpha = 10$ deg case and $\beta = 38$ deg for the $\alpha = 16$ deg case are shown in Figs. 8a and 8b, respectively. In Fig. 8a, interpolated values of both the Horstman and Knight computations are also shown. The abscissa of Figs. 8a and 8b is given as the streamwise distance from the virtual conical origin of the interaction.[1] This was determined from surface-streak patterns in the experiment and from the computational analogs of such patterns. Presenting the results in these coordinates reveals the behavior of c_f in the inception zone of the interaction and in the quasiconical region downstream.

Figure 8a reveals that c_f increases with distance from the virtual origin, eventually asymptoting to a constant level. The measurements and both computations agree on this point, which is entirely consistent with the quasiconical interaction model proposed earlier.[1] Figure 8b shows the same phenomenon in the $\alpha = 16$ deg interaction.

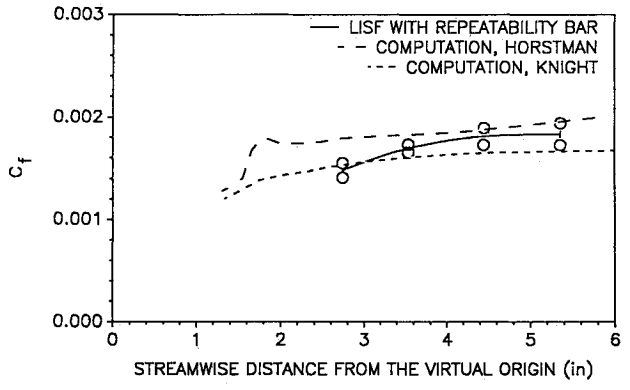

Fig. 8a The c_f distribution along $\beta = 24$ deg conical ray for $\alpha = 10$ deg.

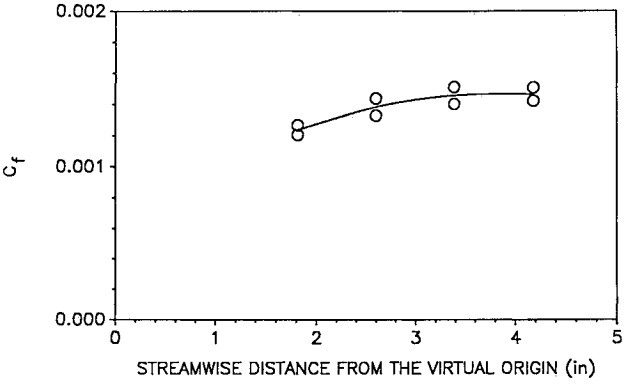

Fig. 8b The c_f distribution along $\beta = 38$ deg conical ray for $\alpha = 16$ deg.

Implications for LISF Measurements in High-shear Flows

As described elsewhere,[9,13,24] surface waves on the oil film impose the most serious limitation on the LISF technique. By disrupting the laser beam, these waves prevent usable interference fringes from being obtained until the oil film becomes quite thin. This effectively limits the number of usable fringes one can obtain, which directly affects the measurement accuracy. The surface-wave problem is exacerbated as τ_w becomes large.

In the present study, we have encountered τ_w levels ranging from 115 to 586 N/m^2. The number of usable fringes we obtained over this range is plotted against τ_w in Fig. 9. This figure indicates that an asymptotic condition of roughly 2 usable fringes may persist even at extremely high shear levels. Actually, the curve fit to the data shown in Fig. 9 yields the expression:

$$N = \frac{1500}{\tau_w} - \frac{58{,}370}{\tau_w^2} \tag{3}$$

but extrapolation of this fit to higher τ_w values is not warranted.

The upshot of Fig. 9 is the following: If sufficient accuracy in c_f can be had from only two interference fringes, then the LISF technique can still be used despite arbitrarily high shear levels. For this reason, we have concentrated our efforts here and in Ref. 13 on extracting the maximum useful information from an extremely limited fringe count. Further details on this and related issues may be found in the doctoral dissertation of Kim.[25]

There appears to be no simple way to increase the fringe count; although switching to a green helium-neon laser ($\lambda = 5230$ Å) or the blue line of an argon-ion laser would produce somewhat of an advantage. The fringe count could be at least doubled by the use of an (invisible) ultraviolet laser, but this approach involves several serious drawbacks.

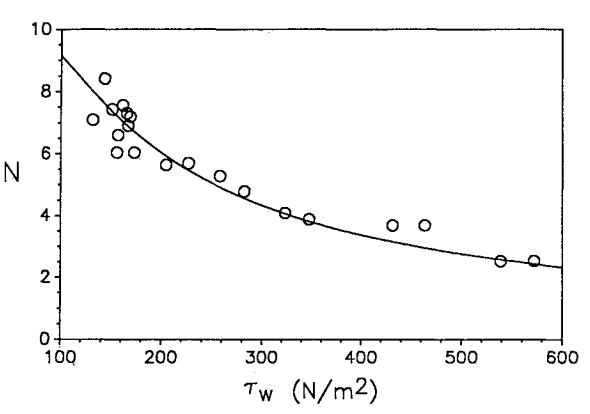

Fig. 9 Number of usable fringes vs shear level.

Conclusions

Experimental measurements have been made of wall shear stresses in swept interactions of a planar shock wave generated by a fin at angle of attack and the 2-D turbulent boundary layer on a flat plate at Mach 3.03. These measurements were made using the LISF meter. The significant conclusions of this study are as follows.

1) The LISF technique is shown to be practical for skin friction measurements in 3-D shock wave/boundary-layer interactions.

2) With proper data acquisition and reduction procedures, the LISF technique is useful even at extremely high wall shear stress levels.

3) In contrast with the case for other skin friction methods, the LISF corrections for pressure and shear gradients are negligible in the present experiment.

4) Skin friction is found to rise at the onset of a weak swept interaction and to reach high levels near the fin for both weak and strong interactions.

5) The present skin friction data, obtained in seven-point ensembles at each measuring station, has an overall repeatability of $\pm 12\%$ or better, based on a 2σ error band.

6) The quasiconical interaction model proposed earlier is supported by the present results.

7) Navier-Stokes computations by two other investigators simulate the overall features and levels of the measured c_f distribution but fail to predict some of the detailed features properly.

Acknowledgments

This research was supported by Air Force Office of Scientific Research Grant 86-0082, monitored by J. D. Wilson. The cooperation of C. C. Horstman and D. D. Knight in making available their computational results and helpful discussions with D. J. Monson and R. V. Westphal are greatly appreciated. The use of data from experiments by F. K. Lu is acknowledged. The development of the Pennsylvania State University LISF meter was supported by NASA Lewis Research Center Grant NAG 3-527, monitored by W. R. Hingst.

References

[1]Settles, G. S. and Dolling, D. S., "Swept Shock Wave/Boundary-Layer Interactions," *AIAA Progress in Astronautics and Aeronautics: Tactical Missile Aerodynamics,* Vol. 104, edited by M. Hemsch and J. Nielsen, AIAA, New York, 1986, pp. 297–379.

[2]"Computational Fluid Dynamics Validation," Report of the Ad Hoc Committee on CFD Validation, Aeronautics Advisory Committee, NASA, May 1, 1987.

[3]Bradshaw, P., Cantwell, B. J., Ferziger, J. H., Kline, S. J., Rubesin, M., and Horstman, C. C., "Experimental Data Needs for Computational Fluid Dynamics—A Position Paper," *Proceedings of the 1980-81-AFOSR-HTTM-Stanford Conference on Complex Turbulent Flows,* Vol. I, edited by S. J. Kline, B. J. Cantwell, and G. M. Lilley, 1981, pp. 23–35.

[4]Winter, K. G., "An Outline of the Techniques Available for the Measurement of Skin Friction in Turbulent Boundary Layers," *Progress in the Aerospace Sciences,* Vol. 18, 1977, pp. 1–57.

[5]Settles, G. S., "Recent Skin Friction Techniques for Compressible Flows," AIAA Paper 86-1099, May 1986.

[6]Tanner, L. H. and Blows, L. G., "A Study of the Motion of Oil Films on Surfaces in Air Flow, with Application to the Measurement of Skin Friction," *Journal of Physics E: Scientific Instruments,* Vol. 9, March 1976, pp. 194–202.

[7]Tanner, L. H., "The Application of Fizeau Interferometry of Oil Films to the Study of Surface Flow Phenomena," *Optics and Lasers in Engineering.,* Vol. 2, 1981, pp. 105–118.

[8]Monson, D. J. and Higuchi, H., "Skin Friction Measurements by a Dual-Laser-Beam Interferometer Technique," *AIAA Journal*, Vol. 19, June 1981, pp. 739–744.

[9]Monson, D. J., Driver, D. M., and Szodruch, J., "Application of a Laser Interferometer Skin-Friction Meter in Complex Flows," *Proceedings of the International Congress on Instrumentation in Aerospace Simulation Facilities,* Sept. 1981, pp. 232–243.

[10]Monson, D. J., "A Nonintrusive Laser Interferometer Method for Measurement of Skin Friction," *Experiments in Fluids,* Vol. 1, 1983, pp. 15–22.

[11]Monson, D. J., "A Laser Interferometer for Measuring Skin Friction in Three-Dimensional Flows," *AIAA Journal,* Vol. 22, April 1984, pp. 557–559.

[12]Westphal, R. V., Bachalo, W. D., and Houser, M. H., "Improved Skin Friction Interferometer," NASA TM 88216, March 1986.

[13]Kim, K.-S. and Settles, G. S., "Skin Friction Measurements by Laser Interferometry," *A Survey of Measurements and Measurement Techniques in Rapidly Distorted Compressible Turbulent Boundary Layers,* edited by H. H. Fernholz, A. J. Smits, and J. P. Dussauge, AGARDograph 315, Nov. 1988, pp. 4.1–4.8.

[14]Lu, F. K., "Fin-Generated Shock-Wave Boundary-Layer Interactions," Ph.D. Thesis, Mechanical Engineering Dept., Pennsylvania State University, University Park, Feb. 1988.

[15]Sun, C. C. and Childs, M. E., "A Modified Wall-Wake Velocity Profile for Turbulent Compressible Boundary Layers," *AIAA Journal of Aircraft,* Vol. 10, June 1973, pp. 318–383.

[16]Van Driest, E. R., "The Problem of Aerodynamic Heating," *Aeronautical Engineering Review,* Vol. 15, Oct. 1956, pp. 26–41.

[17]Settles, G. S. and Teng, H.-Y., "Flow Visualization Methods for Separated Three-Dimensional Shock Wave/Turbulent Boundary Layer Interactions," *AIAA Journal,* Vol. 21, March 1983, pp. 390–397.

[18]Lu, F. K., and Settles, G. S., "Structure of Fin-Shock/Boundary-Layer Interactions by Laser Light-Screen Visualization," AIAA Paper 88-3801, July 1988.

[19]Edney, B. E., "Anomalous Heat Transfer and Pressure Distributions on Blunt Bodies at Hypersonic Speeds in the Presence of an Impinging Shock," Aeronautical Research Inst. of Sweden, Stockholm, FFA Rept. 115, Feb. 1968.

[20]Lu, F. K., Settles, G. S. and Horstman, C. C., "Mach Number Effects on Conical Surface Features of Swept Shock Boundary-Layer Interactions," AIAA Paper 87-1365, June 1987 (to be published in AIAA Journal).

[21]Knight, D. D., Horstman, C. C., Shapey, B. L., and Bogdonoff, S. M., "The Flowfield Structure of the 3-D Shock Wave-Boundary Layer Interaction Generated by a 20 Degree Sharp Fin at Mach 3," AIAA Paper 86-0343, Jan. 1986.

[22]Horstman, C. C., private communication, Oct. 1987.

[23]Knight, D. D., private communication, Oct. 1987.

[24]Murphy, J. D. and Westphal, R. V., "The Laser-Interferometer Skin-Friction Meter—A Numerical and Experimental Study," *Proceedings of the Third Symposium on Numerical and Physical Aspects of Aerodynamic Flows,* Jan. 1985, Paper 7-1.

[25]Kim, K. S., "Skin Friction Measurements by Laser Interferometry in Supersonic Flows," Doctoral Dissertation, Mechanical Engineering Dept., Pennsylvania State University, University Park, Jan. 1989.